



**HAL**  
open science

# Progressively doping graphene with Si: from graphene to silicene, a numerical study

Nathalie Olivi-Tran

► **To cite this version:**

Nathalie Olivi-Tran. Progressively doping graphene with Si: from graphene to silicene, a numerical study. Applied Physics Research, 2015, 7 (6), pp.1. 10.5539/apr.v7n6p1 . hal-01138887v2

**HAL Id: hal-01138887**

**<https://hal.science/hal-01138887v2>**

Submitted on 7 Oct 2015

**HAL** is a multi-disciplinary open access archive for the deposit and dissemination of scientific research documents, whether they are published or not. The documents may come from teaching and research institutions in France or abroad, or from public or private research centers.

L'archive ouverte pluridisciplinaire **HAL**, est destinée au dépôt et à la diffusion de documents scientifiques de niveau recherche, publiés ou non, émanant des établissements d'enseignement et de recherche français ou étrangers, des laboratoires publics ou privés.

# Progressively Doping Graphene with *Si*: from Graphene to Silicene, a Numerical Study

Nathalie Olivi-Tran<sup>1</sup>

<sup>1</sup> Laboratoire Charles Coulomb, Université de Montpellier, CNRS UMR 5221, place Eugene Bataillon, 34095 Montpellier cedex 5, France

Correspondence: Nathalie Olivi-Tran, Laboratoire Charles Coulomb, Université de Montpellier, CNRS UMR 5221, place Eugene Bataillon, 34095 Montpellier cedex 5, France. E-mail: nathalie.olivi-tran@univ-montp2.fr

Received: April 2, 2015 Accepted: April 14, 2015 Online Published: September 24, 2015

doi:10.5539/apr.v7n6p1 URL: <http://dx.doi.org/10.5539/apr.v7n6p1>

## Abstract

For three different sizes of graphene nanosheets, we computed the Density of states when these nanosheets are progressively doped with an increasing percentage of *Si* atoms. The pure graphene nanosheets are semi conducting or not depending on their size. The pure silicene nanosheets are conducting with a conduction due to  $\pi$  electrons. The *Si* doped graphene nanosheets are also semi conducting or not depending on their size: for small sizes, there are semi conducting and they become conducting for larger sizes and larger percentages of *Si* doping. We computed also the total electronic energy which is linked to the mechanical stability of all our nanosheets. This mechanical stability decreases regularly as a function of the *Si* percentage of doping, but for the pure silicene nanosheets, the mechanical stability decreases more abruptly.

**Keywords:** graphene nanosheets, Density of States, *Si*

## 1. Introduction

In recent years, since the isolation of graphene, doping of graphene has become a very important issue (Novoselov 2005; Wehling; 2008). Moreover, the equivalent of graphene for silicon, i.e. silicene is on the way of becoming the next material for electronics. Recently, this graphene analogue, i.e. silicene, has been synthesized on  $ZrB_2(0001)$  thin films (Fleurence, 2012) and on  $Ag(110)$  substrate (De Padova, 2010; De Padova, 2011).

Doping of graphene has been studied for several years now on (Terrones, 2012). The particular case of doping graphene with *Si* leads to several interesting properties like gas sensors (Chen, 2012), catalyst (Chen, 2013). A study has suggested that the synthesized *Si*-doped graphene (Chishlom, 2012) is an effective metal-free catalyst for  $CO$  oxidation (Zhao, 2012). Phase separation of hydrogen atoms adsorbed on graphene has also been studied (Rakhmanov, 2012).

On the other side, silicene is known to be mechanically unstable: silicene has a buckled surface instead of a flat one (Houssa 2010; Kara, 2012). The fact of doping silicene with *C* could enhance its mechanical stability. Recently, a study has shown that *Ni* doped silicene has an increased stability (Manjanath, 2014). Up to now, there has been no study on graphene progressively doped by silicon until obtaining silicene. *Si* and *C* are in the same column of the periodic table, so *Si* when surrounded by *C* can adopt the  $sp^2$  hybridization (Wang, 1987).

We used here a modified tight binding model to compute our Density of States (Olivi-Tran, 1996; Olivi-Tran, 1997; Olivi-Tran 2003). Our computing model has been used several times and has predicted with a very rapid computing time results that were obtained later by ab initio calculations (Verhaegen 1968; Andre, 1971; Leleyter, 1975; Wang 1987; Mishin 2001; Pike 2014). Moreover, this method allows one to obtain electronic characteristics of larger materials than ab initio calculations. It is possible to compute with this method, Density of States of isolated materials, i.e. without substrate and without periodic boundary conditions.

So, we made a numerical study of sheets of graphene of different sizes. The density of states of these sheets and of sheets of graphene doped with 20%, 40%, 60%, 80% of *Si* and of sheets of silicene of the same sizes has been computed. These sheets are isolated, and the doping of our graphene sheets with *Si* atoms is random, i.e. the locations of the *Si* atoms within the graphene sheets is random. The mechanical stability of these different sheets has been also studied.

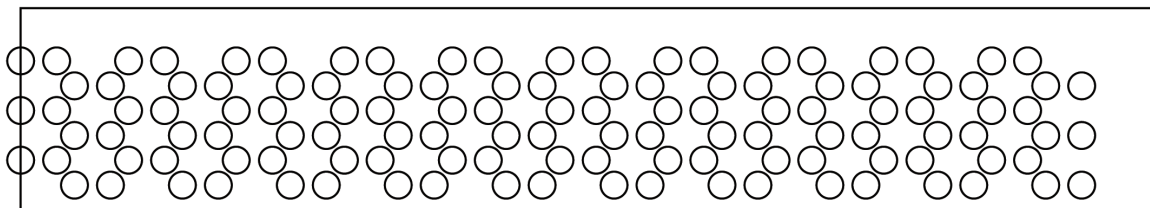


Figure 1. Example of nanosheet of graphene

## 2. Numerical Process

### 2.1 Graphene Sheets Doped with $Si$

We built three sizes of graphene sheets: the first with 120 atoms, then one with 240 atoms and finally one with 480 atoms. Our graphene nanosheets are isolated: there are no substrates and no periodic boundary conditions in the forthcoming computations. An example of graphene sheet is presented in Figure 1. One may see the typical honeycomb structure of this sheet. The carbon structures are then progressively doped with  $Si$  atoms, indeed, we replaced  $C$  atoms in the structure by  $Si$  atoms. This 'doping' is made at random, the silicon atoms have no particular structure with respect to their neighbors, the  $C$  atoms.

These  $Si$  doped graphene sheets are obtained for several percentage of  $Si$  atoms with respect to the total number of atoms in the sheet. This percentages have been set to 0%, 20%, 40%, 60%, 80% and 100%. This last percentage corresponds to a silicene sheet (when all the  $C$  atoms have been replaced by  $Si$  atoms).

So for each size (ranging from 120 to 240) and for each percentage of doping, we computed the density of states of the sheet and the total energy (which gives informations about the mechanical stability of the sheet). 480 atoms is the limit between where one can plot Density of States in a bar plot (because the DOS is discontinuous).

*Calculation of the density of states* This calculation method was initially built for covalent solids with carbon atoms in  $sp^3$  hybridization (cubic diamond lattice). We made this model suitable for finite systems such as nanosheets of group  $IV - B$  elements with possibly including heteroatoms, in the other kinds of hybridization,  $sp$  and  $sp^2$ . In these last cases, the  $p$  bonds are separately treated in the usual Hückel approximation (see below).

Let us recall the main hypotheses. We only consider the four valence atomic orbitals (AO) ( $2s, 2p_i$  for  $C$ ,  $3s, 3p_i$  for  $Si$ ,  $i = x, y, z$ ).

In  $sp^v$  hybridization ( $v = 1, 2, 3$ ), there are four hybrid orbitals per atom ( $C$  or  $Si$ ) built by linear combinations (LCAO) of the above  $s$  and  $p$  AOs, i.e.  $(v + 1)$   $sp$ - or  $\sigma$ -hybrid orbitals along the bond between 2 neighbour atoms, and  $(3 - v)$   $\pi$ -orbitals orthogonal to the bond.

The plane geometries (2D) can be studied in  $sp^2$  hybridization.

The partition of the Hamiltonian is valid since we are in the "one-electron approximation", and leads to two independent Hamiltonians:  $sp$  Hamiltonian and  $p$  Hamiltonian. The Hamiltonians are given below.

The  $\sigma$  or  $sp$  Hamiltonian describes the skeleton of the cluster bonds.

The  $\pi$  Hamiltonian is dealing with delocalized electrons:  $\pi$  AOs are perpendicular to the molecular plane if it is a 2D-molecule.

The electronic energy of a cluster is deduced by diagonalizing the Hamiltonians and filling in the energy levels with all the valence electrons. The origin of the energies is taken as usual at the vacuum level.

However, an important restriction has to be brought: in our model indeed, neither the repulsive energies between the nuclei nor the dielectronic correlations are clearly taken into account. In fact, averaged values of these contributions are included in the parameters of the model such as  $\beta_\sigma$  or  $\beta_\pi$ , the usual resonance integrals used in the Hamiltonians. Nevertheless, the results of our calculations are validated by comparison to the results of ab initio calculations on some very small clusters (Verhaegen, 1968; Leleyter, 1975).

Due to this restriction, in order to determine which clusters are the most stable ones for a given number of atoms  $n$ , we are only able to compare the electronic energies of clusters with the same number of bonds.

The silicon atoms are assumed to be in the same hybridization as the surrounding carbon atoms.

Let us remind that this is a one electron model, each electron moves in a mean potential  $V(r)$  which represents both the nuclei attraction and the repulsion of other electrons.  $\sigma$  and  $\pi$  electrons are separately treated :

With  $|iJ\rangle$  : hybrid  $sp^\nu$  orbital ( $\nu = 1, 2, 3$ ) which points from site  $i$  along the bond  $J$ . The molecular orbital  $\sigma$  is given by:

$$|\Psi\rangle = \sum_{i,J} a_{iJ} |iJ\rangle \quad (1)$$

So, the energy origin taken at the vacuum level, the Hamiltonian can be written as:

$$H_\sigma = E_m \sum_{i,J} |iJ\rangle \langle iJ| + \Delta_\sigma \sum_{i,J,J' \neq J} |iJ\rangle \langle iJ'| + \beta_{\text{sigma}} \sum_{i,i' \neq i,J} |iJ\rangle \langle i'J| \quad (2)$$

( $i$  and  $i'$  are first neighbours) where  $E_m$  is the average energy:  $E_m = (E_s - \nu E_p)/(\nu + 1)$ ,  $E_s$  and  $E_p$  are the atomic level energies,  $\beta_\sigma$  is the usual hopping or resonance integral in Hückel theory (interaction between nearest neighbour atoms along the bond),  $\Delta_\sigma$  is a promotion integral (transfer between hybrid orbitals on the same site) :  $\nu = (E_s - E_p)/(\nu + 1)$ .

Remark: for an infinite crystal (bulk), the gap between valence and conduction band (forbidden band) is  $g = |-2\nu + (\nu + 1)\nu|$  (for IVB elements) and  $\beta_\sigma$  can be derived from the values of  $g$  (5.33 eV for C, 1.14 for Si).

The Hamiltonian of  $\pi$  bonds writes:

$$H_\pi = E_p \sum_i |i\rangle \langle i| + \beta_\pi \sum_{i,i' \neq i} |i\rangle \langle i'| \quad (3)$$

with  $|i\rangle$  :  $\pi$  orbital centered on atom  $i$ ,  $\beta_\pi$  : hopping integral for  $\pi$  levels.

The  $\beta_\pi$  value for C was chosen in order to get the correct positions of  $C_2$  energy levels in comparison to the results of the Verhaegens ab initio calculation (Verhaegen, 1968).

We need only 3 parameters:  $\beta_\sigma$ ,  $\beta_\pi$  and  $\Delta_\sigma$  for the homonuclear model which represent in fact the average potential  $V(r)$  and which take into account the nuclear attraction and the dielectronic interactions (Leleyter, 1975). But due to the fact that we only take into account on average the nuclear and dielectronic interactions, we can only compare clusters with the same number of atoms and the same number of bonds.

Table 1. Tight binding parameters (Verhaegen, 1968)

$sp^2$	C	Si
$E_s$ (eV)	-19.45	-14.96
$E_p$ (eV)	-10.74	-7.75
$\beta_\sigma$ (eV)	-7.03	-4.17
$\beta_\pi$ (eV)	-3.07	-0.8
$\Delta_\sigma$ (eV)	-2.90	-2.40

As a summary, we used a semi-empirical method which is validated by the comparison with ab initio computations or Density Functional Theory computations, but which is infinitely faster due to the very small number of parameters which are necessary (Verhaegen, 1968; Andre, 1971; Leleyter, 1975; Wang, 1987; Mishin, 2001; de Souza Martins, 2014). This method may lead to the study of the more stable geometries. The tight binding model (or Hckel model) has been used for small metal clusters and gave similar results to those of local-spin-density and configuration interaction calculations (Wang, 1987).

### 3. Results and Discussion

Figures 2 and 3 show the density of states, DOS, (in arbitrary units) for nanosheets of graphene doped with Si. The percentage of doping ranges from 0% (top graph) to 100% of Si atoms. These nanosheets of C doped with Si have a size of 120 atoms. For all DOS graphs, 0 is the vacuum level.

In the top graph corresponding to 0% of Si doping, we see that there is a gap of  $1.5eV \pm 0.5$ : graphene is semi-conducting within these conditions: boundary conditions and isolation of the nanosheet. We see that, comparing with an infinite  $sp^3$  hybridized crystal, the gap is narrowed ( $1.5eV$  compared to  $5.33eV$  see above).

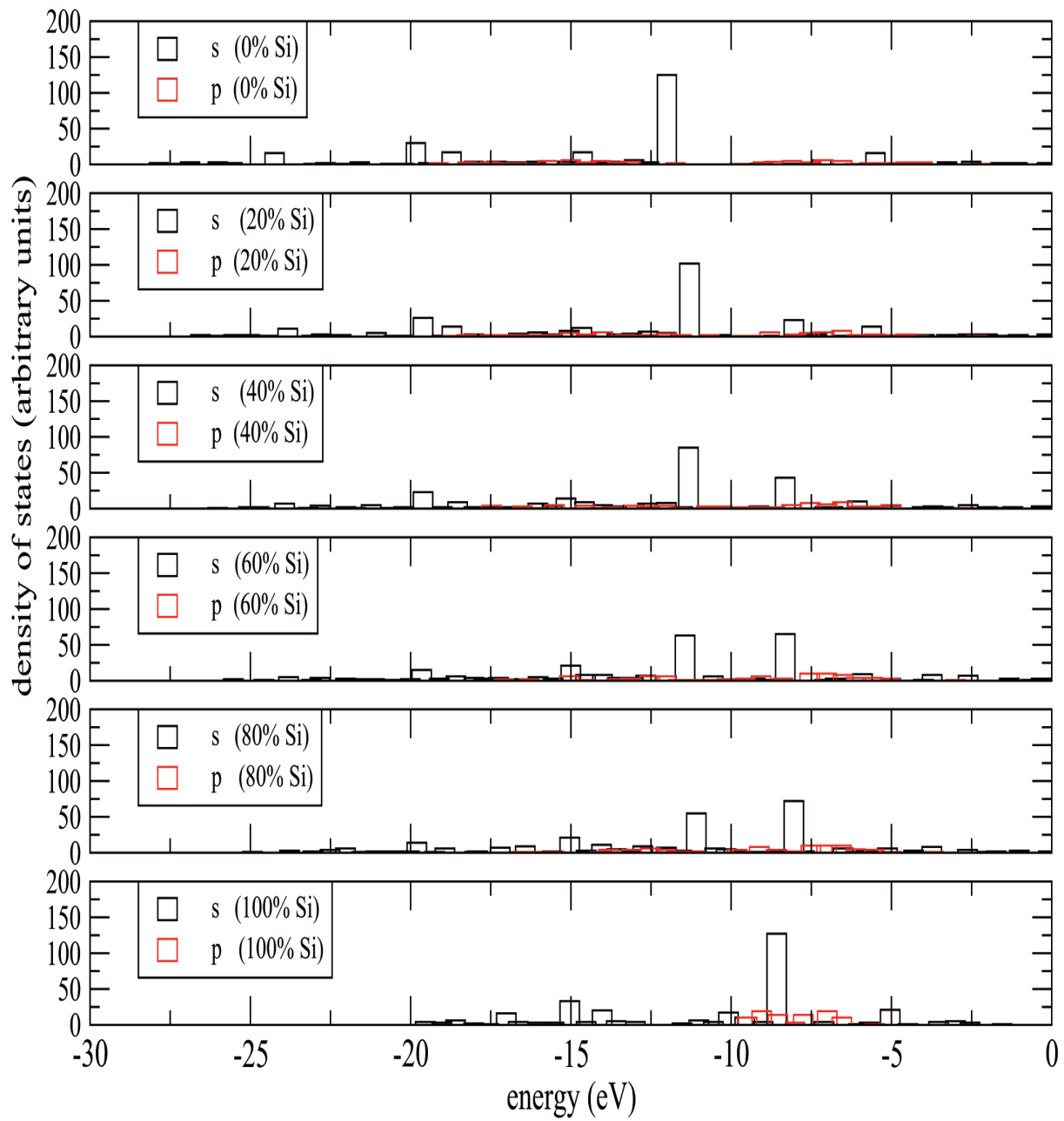


Figure 2. Total DOS of nanosheets containing 120 atoms. From top to bottom: graphene nanosheets doped with 0%, 20%, 40%, 60%, 80% and 100% of *Si* atoms-the width of the bars corresponds to the error bar

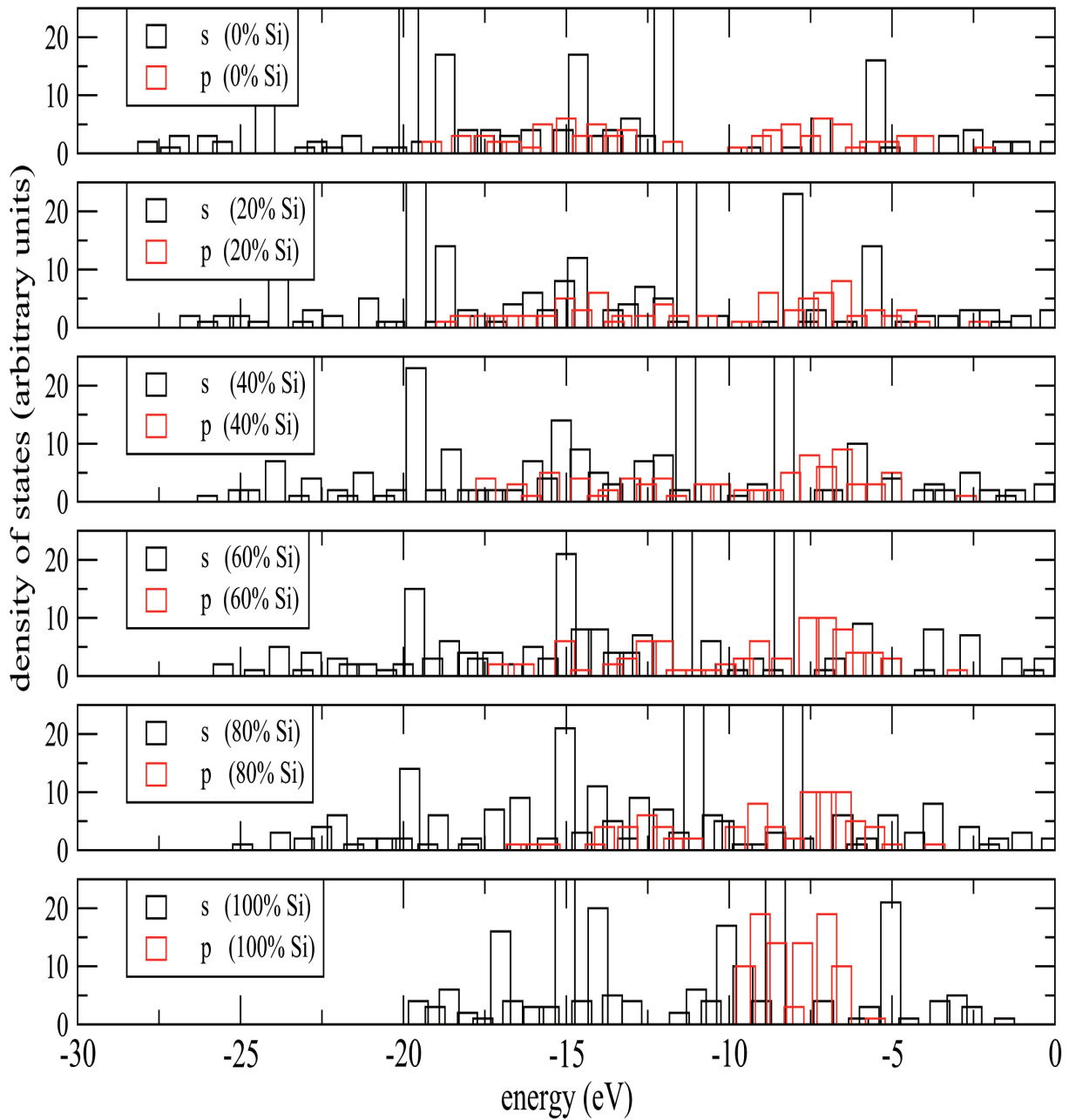


Figure 3. Details of DOS of nanosheets containing 120 atoms. From top to bottom: graphene nanosheets doped with 0%, 20%, 40%, 60%, 80% and 100% of *Si* atoms the width of the bars corresponds to the error bar

Located at  $-11.5 \pm 0.5 eV$  on the DOS, there is a peak which corresponds to Highest Occupied Molecular Orbital (HOMO) for *C* nanosheets. When increasing the amount of *Si* atoms within the structure of the nanosheet (top graph to bottom), we see that this peak remains but decreases in intensity and another peak appears at  $-7 \pm 0.5 eV$  which corresponds to the HOMO for *Si* nanosheets. So the value of the HOMO in doped graphene nanosheets decreases with the increase of *Si* doping.

The bottom graph which corresponds to a pure silicene nanosheet is also semi conducting with a gap of  $1 \pm 0.5 eV$ . Compared to a bulk  $sp^3 Si$  crystal, the gap is narrower ( $1.14 eV$  in a bulk crystal, see above). This semi-conducting feature may be due to the small number of atoms contained in the nanosheet.

The intermediate doped nanosheets (ranging from 20% to 80% *Si* doped nanosheets) are first semi conducting for low *Si* doping then become conducting for larger *Si* doping. For all nanosheets containing 120 atoms and *C* atoms (corresponding to all the graphs of Figures 2 and 3 except the bottom graph), the DOS is relatively wide when comparing to the DOS of the pure silicene nanosheet (bottom graph): the DOS for a pure silicene nanosheet is more degenerate than the DOS for *Si* doped graphene nanosheets.

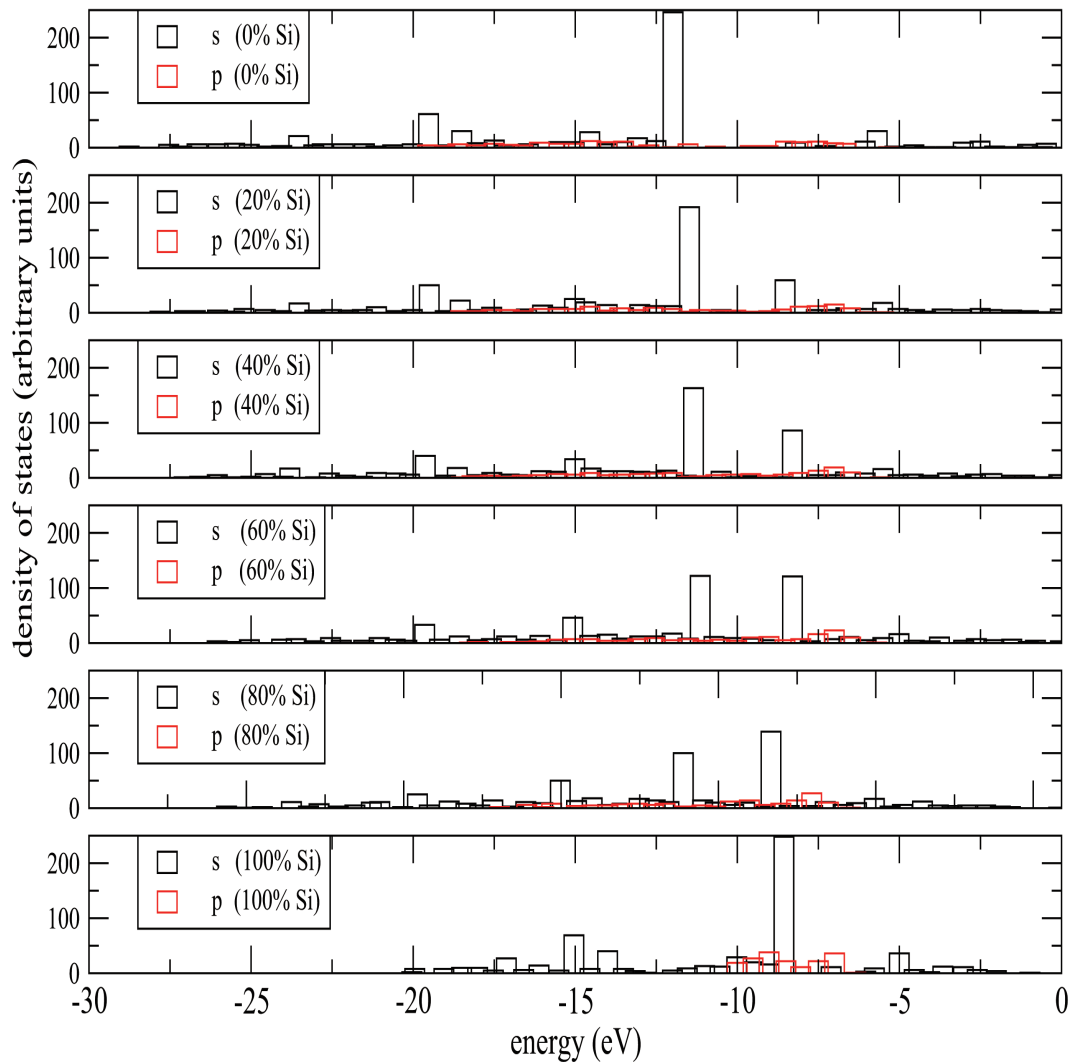


Figure 4. Total DOS of nanosheets containing 240 atoms. From top to bottom: graphene nanosheets doped with 0%, 20%, 40%, 60%, 80% and 100% of *Si* atoms-the width of the bars corresponds to the error bar

Figures 4 and 5 show the density of states, DOS, (in arbitrary units) for nanosheets of graphene doped with *Si*. The percentage of doping ranges from 0% (top graph) to 100% of *Si* atoms. These nanosheets of *C* doped with *Si* have a size of 240 atoms.

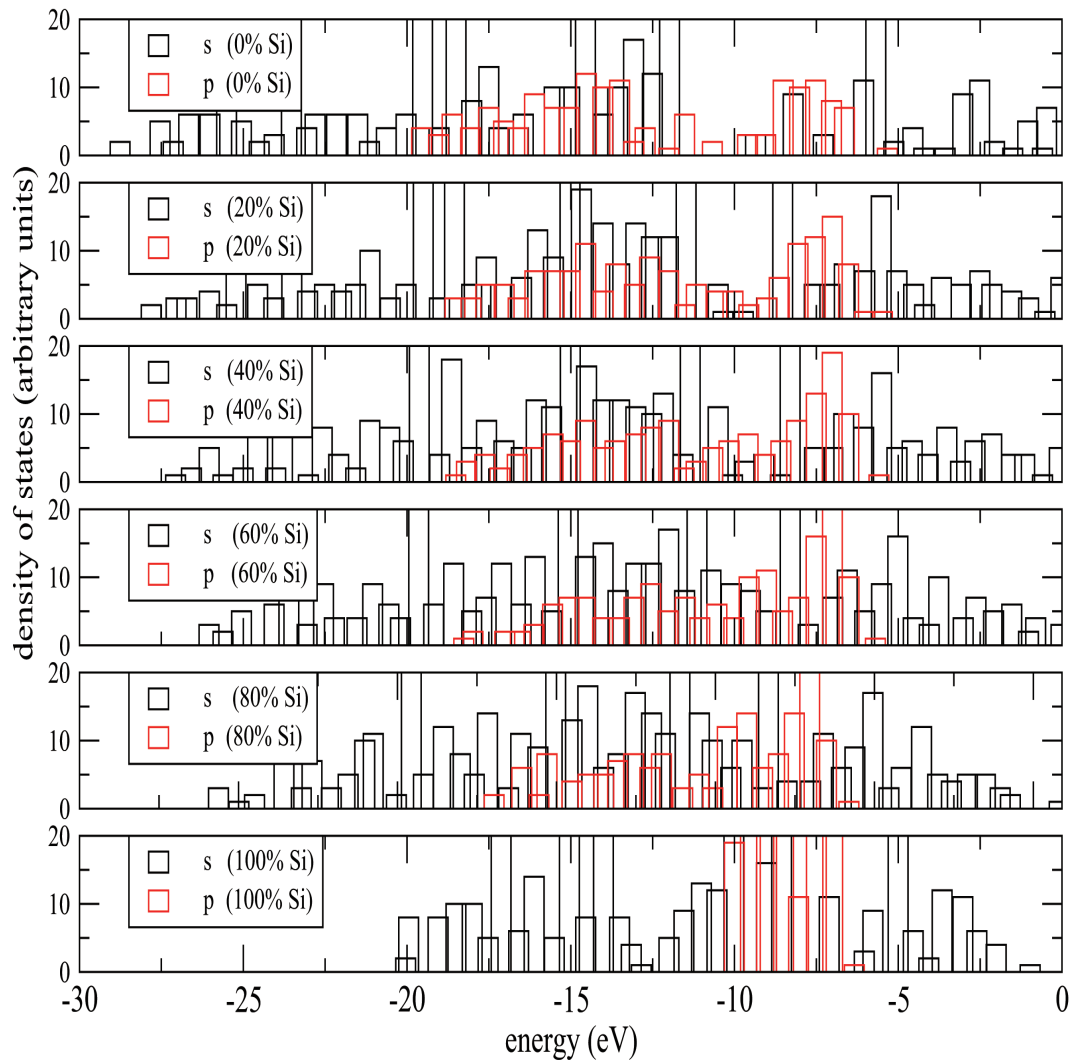


Figure 5. Details of DOS of nanosheets containing 240 atoms. From top to bottom: graphene nanosheets doped with 0%, 20%, 40%, 60%, 80% and 100% of  $Si$  atoms-the width of the bars corresponds to the error bar

Contrarily to the DOS of the nanosheets of 120 atoms, there is no gap for the pure  $C$  graphene nanosheet (top graph) as well as for the pure  $Si$  silicene nanosheet (bottom graph). Let us notice that in the top graph, one may see two gaps in the  $-12eV - 10eV$  region, but as the error margin is equal to  $0.5eV$ , those intervals are not real gaps in the conductivity. It is well known, furthermore, that the conductivity of graphene depends on several characteristics: boundary conditions, size of the nanosheets, doping of the graphene nanosheets etc.

The same peaks in the DOS appear like in Figures 2 and 3: the HOMO  $C$  nanosheets peak and the HOMO  $Si$  nanosheets peak. So we can say that, like graphene, the semi conducting or conducting character of silicene depends on the size of the nanosheet; indeed, for a small size (120 atoms) the DOS of the pure silicene nanosheet shows a small gap.

In Figure 5, the  $Si$  doped nanosheets are all conducting, there is no gap within their DOS (intermediate graphs of Figure 5, between top and bottom). Moreover, the width of the pure  $Si$  silicene nanosheet DOS is narrower than the DOS of nanosheets containing  $C$  atoms.

Figures 6 and 7 show the density of states, DOS, (in arbitrary units) for nanosheets of graphene doped with  $Si$ . The percentage of doping ranges from 0% (top graph) to 100% of  $Si$  atoms (bottom graph). These nanosheets of  $C$  doped with  $Si$  have a size of 480 atoms.



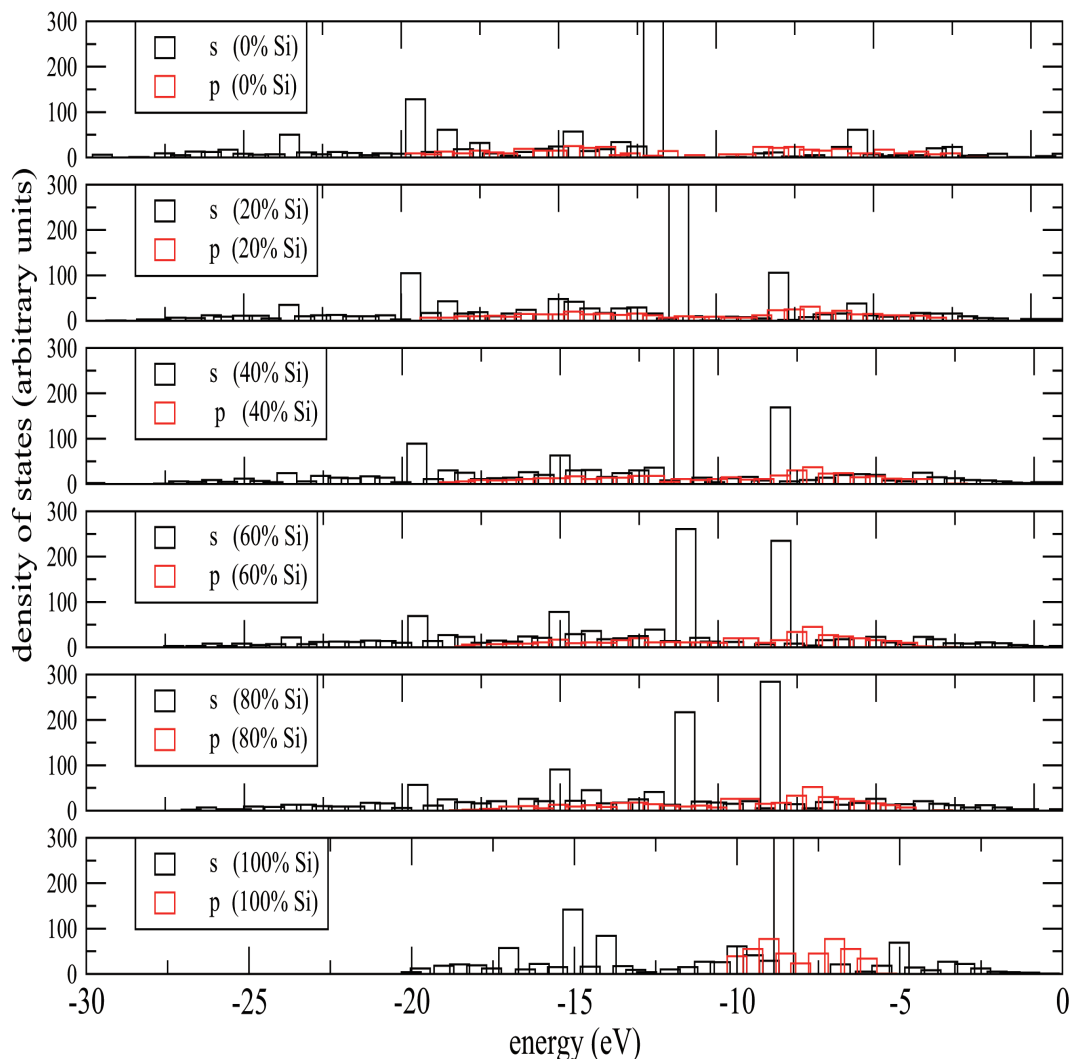


Figure 6. Total DOS of nanosheets containing 480 atoms. From top to bottom: graphene nanosheets doped with 0%, 20%, 40%, 60%, 80% and 100% of  $Si$  atoms—the width of the bars corresponds to the error bar

Like for nanosheets of 240 atoms, there is no gap in all the DOS presented in Figure 6. In the top graph (for a pure graphene nanosheet) the error margin is  $\pm 0.5eV$  so what may be seen as a gap is in fact the characteristic DOS of a conducting nanosheet.

Once again (like in Figures 2,3,4,5), the HOMO peak for pure graphene nanosheets, appears at  $-11.5 \pm 0.5eV$  in the top graph. For doping increasing from 20% to 100%, this peak disappears and the HOMO peak for pure  $Si$  nanosheets appears at about  $-7.5 \pm 0.5eV$ .

Now comparing Figures 2, 3,4,5,6 and 7, one may see that the pure graphene nanosheet is conducting or not depending on the size of the nanosheet: for a small nanosheet (120 atoms), there is a gap which disappears for larger numbers of atoms in the nanosheet. Indeed, for 240 atoms and 480 atoms, the graphene nanosheets are conducting.

In all the 6 figures, the DOS for the pure silicene nanosheets are narrower, as well for the  $\sigma$  DOS (in black) as for the  $\pi$  DOS (in red). The  $\pi$  DOS in this case, covers the gap in the  $\sigma$  DOS.

For nanosheets doped with 20% to 80% of  $Si$  atoms, the conduction is made by both  $\pi$  and  $\sigma$  electrons. While for the pure  $Si$  and for the pure  $C$  nanosheets (240 and 480 atoms), the conduction comes only from the  $\pi$  electrons. One recovers the conducting character of pure, isolated silicene nanosheets.

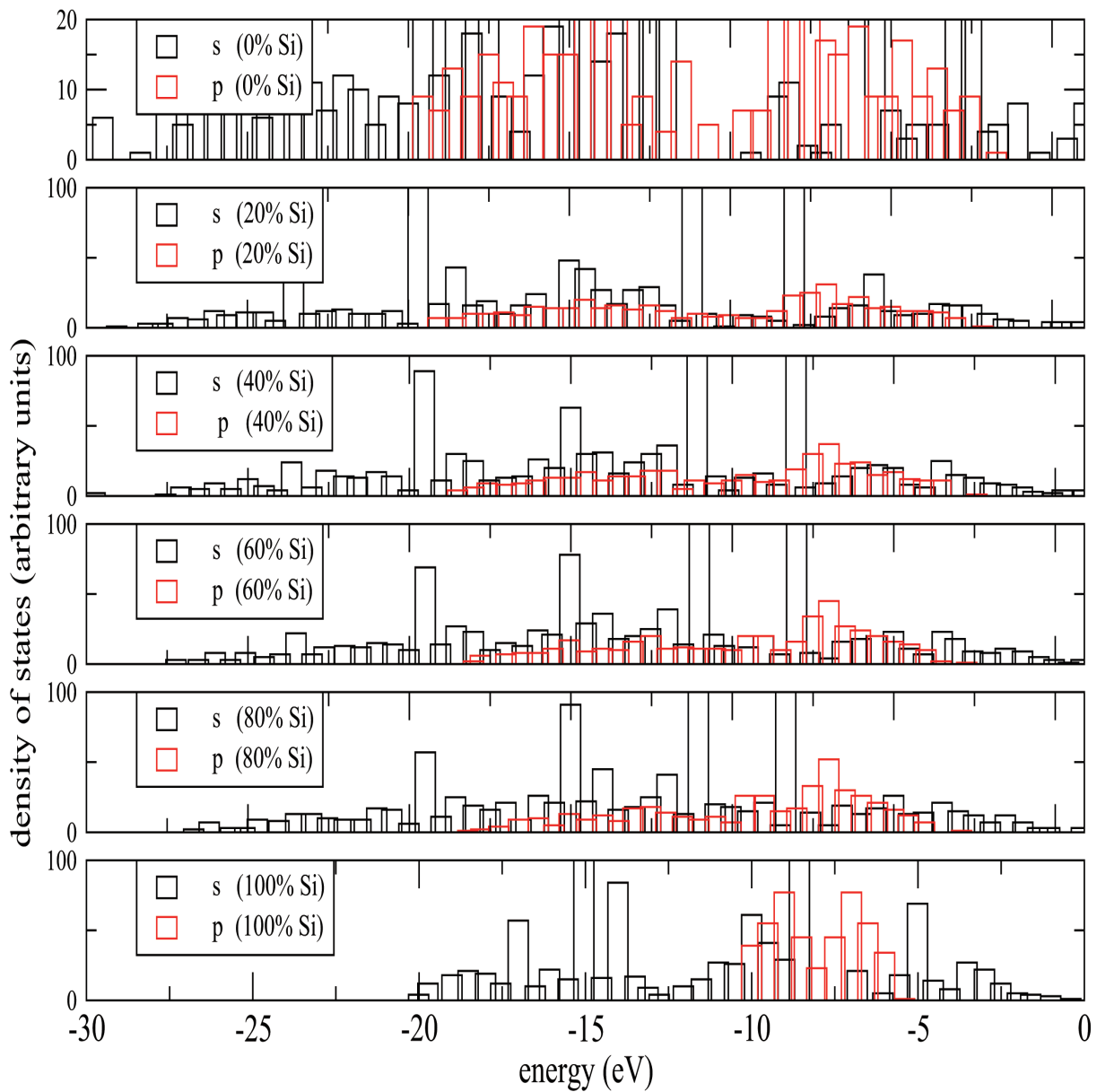


Figure 7. Details of DOS of nanosheets containing 480 atoms. From top to bottom: graphene nanosheets doped with 0%, 20%, 40%, 60%, 80% and 100% of *Si* atoms-the width of the bars corresponds to the error bar

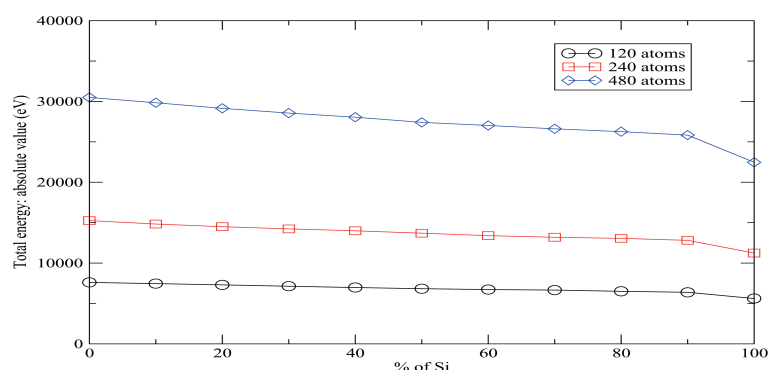


Figure 8. Absolute value of the total electronic energy as a function of the percentage of doping with *Si* atoms, for graphene nanosheets of 120,240 and 480 atoms

Figure 8 is the total electronic energy as a function of the percentage of *Si* atoms within the nanosheets. This total electronic energy shows the mechanical stability of the studied nanosheets because it is linked to the strength of the covalent bonds (Olivi-Tran, 2010). We see that as the total electronic energy is decreasing in absolute value, the mechanical stability is decreasing. This decreasing is slow for nanosheets containing *C* atoms and the decreasing accelerates for pure silicene nanosheets. This may be explained by the fact that in the pure *Si* nanosheets, the  $\pi$  electrons induce a buckled surface. So even with a high percentage of *Si* atoms within the nanosheet, the mechanical stability is higher because the  $\pi$  electrons cannot interact over the whole surface.

#### 4. Conclusion

We studied the Density of States of graphene nanosheets doped with *Si* atoms until obtaining pure silicene nanosheets. The DOS depend both on the sizes of the nanosheets and on the doping percentage. There is an abrupt change in the DOS for pure and doped graphene nanosheets compared to the pure silicene nanosheets. This abrupt change may be also seen in the total electronic energy which is linked to the mechanical stability of our nanosheets: when reaching 100% of *Si* atoms composing the nanosheet, the mechanical stability decreases abruptly compared to nanosheets containing only 20% of *C* atoms. This study opens a new way for semi conducting and nanoelectronic devices as it is easier to obtain graphene nanosheets with impurities than pure graphene or silicene nanosheets.

#### Reference

- Andr, J. M., Kapsomenos, G. S., & Leroy, G. (1971). A comparison of ab initio, extended Hckel and CNDO band structures for polyene and polyethylene. *Chemical Physics Letters*, 8(2), 195-197.
- Chen, Y., Gao, B., Zhao, J. X., Cai, Q. H., & Fu, H. G. (2012). Si-doped graphene: an ideal sensor for NO-or NO<sub>2</sub>-detection and metal-free catalyst for N<sub>2</sub>O-reduction. *Journal of molecular modeling*, 18(5), 2043-2054. <http://dx.doi.org/10.1007/s00894-011-1226-x>
- Chen, Y., Liu, Y. J., Wang, H. X., Zhao, J. X., Cai, Q. H., Wang, X. Z., & Ding, Y. H. (2013). Silicon-doped graphene: an effective and metal-free catalyst for NO reduction to N<sub>2</sub>O?. *ACS applied materials & interfaces*, 5(13), 5994-6000. <http://dx.doi.org/10.1021/am400563g>
- Chisholm, M. F., Duscher, G., & Windl, W. (2012). Oxidation resistance of reactive atoms in graphene. *Nano letters*, 12(9), 4651-4655. <http://dx.doi.org/10.1021/nl300897m>
- De Padova, P., Quaresima, C., Olivieri, B., Perfetti, P., & Le Lay, G. (2011). sp<sup>2</sup>-like hybridization of silicon valence orbitals in silicene nanoribbons. *Applied Physics Letters*, 98(8), 081909. <http://dx.doi.org/10.1063/1.3557073>
- De Padova, P., Quaresima, C., Ottaviani, C., Sheverdyayeva, P. M., Moras, P., Carbone, C., ... & Le Lay, G. (2010). Evidence of graphene-like electronic signature in silicene nanoribbons. *Applied Physics Letters*, 96(26), 261905. <http://dx.doi.org/10.1063/1.3459143>
- de Souza Martins, A., & Verssimo-Alves, M. (2014). Group-IV nanosheets with vacancies: a tight-binding extended Hckel study. *Journal of Physics: Condensed Matter*, 26(36), 365501. <http://dx.doi.org/10.1088/0953->

8984/26/36/365501

- Fleurence, A., Friedlein, R., Ozaki, T., Kawai, H., Wang, Y., & Yamada-Takamura, Y. (2012). Experimental evidence for epitaxial silicene on diboride thin films. *Physical review letters*, 108(24), 245501. <http://dx.doi.org/10.1103/PhysRevLett.108.245501>
- Houssa, M., Pourtois, G., Afanas' Ev, V. V., & Stesmans, A. (2010). Can silicon behave like graphene? A first-principles study. *Applied Physics Letters*, 97(11), 112106. <http://dx.doi.org/10.1063/1.3489937>
- Kara, A., Enriquez, H., Seitsonen, A. P., Voon, L. L. Y., Vizzini, S., Aufray, B., & Oughaddou, H. (2012). A review on silicene: a new candidate for electronics. *Surface science reports*, 67(1), 1-18. <http://dx.doi.org/10.1016/j.surfrep.2011.10.001>
- Leleyter, M., & Joyes, P. (1975). Étude expérimentale et théorique de l'émission secondaire d'ions moléculaires. Cas des éléments du groupe IV-B. *Journal de Physique*, 36(5), 343-355. <http://dx.doi.org/10.1051/jphys:01975003605034300>
- Manjanath, A., Kumar, V., & Singh, A. K. (2014). Mechanical and electronic properties of pristine and Ni-doped Si, Ge, and Sn sheets. *Physical Chemistry Chemical Physics*, 16(4), 1667-1671. <http://dx.doi.org/10.1039/C3CP54655A>
- Mishin, Y., Mehl, M. J., Papaconstantopoulos, D. A., Voter, A. F., & Kress, J. D. (2001). Structural stability and lattice defects in copper: Ab initio, tight-binding, and embedded-atom calculations. *Physical Review B*, 63(22), 224106. <http://dx.doi.org/10.1103/PhysRevB.63.224106>
- Novoselov, K. S. A., Geim, A. K., Morozov, S., Jiang, D., Katsnelson, M., Grigorieva, I., ... & Firsov, A. (2005). Two-dimensional gas of massless Dirac fermions in graphene. *Nature*, 438(7065), 197-200. DOI : 10.1038/nature04233
- Olivi-Tran, N., & Leleyter, M. (1996). Electronic structure of a fractal cluster of carbon atoms in the hybridization calculated by the Hckel method. *Journal of Physics: Condensed Matter*, 8(24), 4361. <http://dx.doi.org/10.1088/0953-8984/8/24/005>
- Olivi-Tran, N., & Leleyter, M. (2003). Silica fractal atomic clusters saturated with OH. *Chaos, Solitons & Fractals*, 17(5), 819-824. [http://dx.doi.org/10.1016/S0960-0779\(02\)00323-5](http://dx.doi.org/10.1016/S0960-0779(02)00323-5)
- Olivi-Tran, N., Ferchichi, A., Calas, S., & Etienne, P. (2010). Total electronic energy by tight binding approximation and experimental toughness of three different hybrid polymers. *Journal of Non-Crystalline Solids*, 356(6), 287-289. <http://dx.doi.org/10.1016/j.jnoncrysol.2009.12.009>
- Olivi-Tran, N., Leleyter, M., & Thouy, R. (1997). Electronic spectral dimension of a fractal aggregate taking account of hybridization. *Journal of Physics: Condensed Matter*, 9(14), L225-L229. <http://dx.doi.org/10.1088/0953-8984/9/14/001>
- Pike, N. A., & Stroud, D. (2014). Tight-binding model for adatoms on graphene: Analytical density of states, spectral function, and induced magnetic moment. *Physical Review B*, 89(11), 115428. DOI : 10.1103/PhysRevB.89.115428
- Rakhmanov, A. L., Rozhkov, A. V., Sboychakov, A. O., & Nori, F. (2012). Phase separation of hydrogen atoms adsorbed on graphene and the smoothness of the graphene-graphane interface. *Physical Review B*, 85(3), 035408. DOI : 10.1103/PhysRevB.85.035408
- Terrones, H., Lv, R., Terrones, M., & Dresselhaus, M. S. (2012). The role of defects and doping in 2D graphene sheets and 1D nanoribbons. *Reports on Progress in Physics*, 75(6), 062501. <http://dx.doi.org/10.1088/0034-4885/75/6/062501>
- Verhaegen, G. (1968). Theoretical calculation of the electronic states of C<sub>2</sub><sup>+</sup>. *The Journal of chemical physics*, 49(10), 4696-4705. <http://dx.doi.org/10.1063/1.1669932>
- Wang, Y., George, T. F., Lindsay, D. M., & Beri, A. C. (1987). The Hckel model for small metal clusters. I. Geometry, stability, and relationship to graph theory. *J. Chem. Phys.*, 86, 3493-9. <http://dx.doi.org/10.1063/1.452005>
- Wehling, T. O., Novoselov, K. S., Morozov, S. V., Vdovin, E. E., Katsnelson, M. I., Geim, A. K., & Lichtenstein, A. I. (2008). Molecular doping of graphene. *Nano letters*, 8(1), 173-177. <http://dx.doi.org/10.1021/nl072364w>
- Zhao, J. X., Chen, Y., & Fu, H. G. (2012). Si-embedded graphene: an efficient and metal-free catalyst for CO

oxidation by N<sub>2</sub>O or O<sub>2</sub>. *Theoretical Chemistry Accounts*, 131(6), 1-11.<http://dx.doi.org/10.1007/s00214-012-1242-7>

### **Copyrights**

Copyright for this article is retained by the author(s), with first publication rights granted to the journal.

This is an open-access article distributed under the terms and conditions of the Creative Commons Attribution license (<http://creativecommons.org/licenses/by/3.0/>).